

Operational Evapotranspiration Estimates from SEVIRI support Sustainable Water Management

George P. Petropoulos^{1*}, Gareth Ireland¹, Salim Lamine^{1,2}, Hywel M. Griffiths¹,
Nicholas Ghilain³, Vasilieios Anagnostopoulos⁴, Matthew R. North¹,
Prashant K. Srivastava^{5,6}, Hro Georgopoulou⁷

¹ Department of Geography and Earth Sciences, Aberystwyth University, Aberystwyth, SY23 2DB, Wales, UK

² Department of Ecology and Environment, University of Sciences and Technology Houari Boumediene, BP 32, El Alia, Bab
Ezzouar, Algiers, Algeria

³ Royal Meteorological Institute, Brussels, Belgium

⁴ Distributed and Knowledge Management Systems Lab, National Technical University of Athens, Greece

⁵ NASA Goddard Space Flight Center, Greenbelt, Maryland, USA

⁶ Institute of Environment and Sustainable Development, Banaras Hindu University, Varanasi, India

⁷ InfoCosmos Ltd, Pindou 71, 13341, Athens, Greece

* Author for correspondence, email: petropoulos.george@gmail.com

ABSTRACT

This study aimed at exploring the accuracy of the Evapotranspiration (ET) operational estimates from the Meteosat Second Generation (MSG) Spinning Enhanced Visible Infra-Red Imager (SEVIRI) at a range of selected ecosystems in Europe. For this purpose were utilised *in-situ* eddy covariance measurements acquired from 7 selected experimental sites belonging to the CarboEurope ground observational network, acquired over 2 full years of observations (2010-2011). Appraisal of ET accuracy from this product was also investigated with respect to land cover, season and each site(s) degree of heterogeneity, the latter being expressed by the fractional vegetation cover (FVC) operational product of SEVIRI.

Results indicated a close agreement between the operational products ET estimates and the tower based *in-situ* ET measurements for all days of comparison, showing a satisfactory correlation (r of 0.709) with accuracies often comparable to previous analogous studies. From all land cover types, the grassland and cropland sites exhibited the closest agreement (r from 0.705 to 0.759). Among seasons, strongest correlations were observed during the summer and autumn (r of 0.714 & 0.685 respectively), whereas with FVC a highest correlation of 0.735 was observed for the class FVC 0.75-1 when compared against the observed values for the complete monitoring period. Our findings support the potential value of the SEVIRI ET product for regional to mesoscale studies and corroborate its credibility for usage in many practical applications. The latter is of particular importance for water limiting environments, such as those found in the Mediterranean basin, as accurate information on ET rates can provide tremendous support in sustainable water resource management as well as policy and decision making in those areas.

KEYWORDS: *evapotranspiration, ET, SEVIRI, water management, Earth Observation, CarboEurope*

44 1. INTRODUCTION

45 The combined impacts of climate change, population increase and migration to urban areas are
46 likely to cause significant water resource crises in the coming decades (Jones, 2014). The
47 temporal and spatial scales of these crises mean that mitigation of, and adaptation to them,
48 require reliable data on which management decisions can be made (Wagner *et al.*, 2015).
49 However, these data are lacking for a number of important hydrological processes, especially in
50 regions such as Africa (Legesse *et al.*, 2003) South America (Smolders *et al.*, 2004) and Asia
51 (Remesan and Holman, 2015; Srinivasan *et al.*, 2015). One such process which is of key
52 importance in many practical applications is evapotranspiration (Srivastava *et al.*, 2013c;
53 Ireland *et al.*, 2015). This critical process is the way in which water is transferred as vapour from
54 the terrestrial and marine environments into the atmosphere and is principally influenced by
55 meteorological factors and soil moisture availability (Srivastava *et al.*, 2013a; Sepulcre-Canto *et al.*,
56 2014). As such, it is central to the hydrological cycle as well as to hugely significant
57 biogeochemical cycles (in particular carbon), and is the main pathway of the energy system by
58 which solar energy is transferred through latent heat (LE). As a result, its importance as a
59 control on regional climate characteristics (Jung *et al.*, 2010; Srivastava *et al.*, 2015c), agriculture
60 and regional water resources cannot be understated (Buytaert *et al.*, 2006; Srivastava *et al.*,
61 2013b; Srivastava *et al.*, 2015b).

62 There is a long history of ground surface-based instrumental retrieval of ET using a number of
63 techniques, including evaporation pans, atmometers and lysimeters (for a review see
64 (Petropoulos *et al.*, 2013). Such techniques are limited by the fact that they are often used in
65 single sites and are also unable to provide spatiotemporal estimates of ET at regional or
66 continental scales. In recent years there a number of ground monitoring networks have been
67 developed (e.g. Fluxnet) in order to integrate data collected at single sites around the world
68 (Wang and Dickinson, 2012). However, the development of regional estimates of ET remain
69 limited by the cost of instrumentation implementation and the fact that such measurements are
70 time-consuming and labour intensive.

71 The advent of Earth Observation (EO) technology has led to the development of a number of
72 modelling techniques which have been proposed to obtain spatiotemporal estimates of ET (Sun
73 *et al.*, 2011; Gellens-Meulenberghs *et al.*, 2012; Marshall *et al.*, 2013; Cruz-Blanco *et al.*, 2014;
74 Ghilain *et al.*, 2014). Some studies of ET have also been performed on European ecosystems
75 using mesoscale model derived weather variables (Verstraeten *et al.*, 2005; Srivastava *et al.*,
76 2014; Srivastava *et al.*, 2015d) as well as satellites such as MODIS (Srivastava *et al.*, 2015a),
77 SEVIRI (Petropoulos *et al.*, 2015a), and AVHRR (Taconet *et al.*, 1986). In contrast to conventional
78 ground surface-based methods, these methods can provide maps of ET at varying spatial and
79 temporal resolutions and at relatively low or often no cost. Yet, before such EO-derived maps are
80 used, it is essential to undertake validation studies for a number of reasons (Jia *et al.*, 2010;
81 Petropoulos *et al.*, 2013), including: (i) to determine the suitability and credibility of an EO
82 algorithm or operational product before it is used for practical applications; (ii) to allow for the
83 identification, quantification and understanding of the sources of errors in algorithm
84 formulation and (iii) to direct efforts to re-evaluate and improve ET retrieval parameters and
85 algorithm structure. These reasons allow environmental managers, regulatory agencies and
86 disaster management agencies to use the product with greater confidence and also, crucially,
87 allow for climate change projections to be evaluated (Mueller *et al.*, 2011; Kalivas *et al.*, 2013).

88 EO technology is currently at a level of maturity which allows the development and distribution
89 of related products at operational scales. Such operational products have proven to be generally

90 of high demand from research groups and communities interested in modelling the carbon cycle,
91 understanding the relationships between fire regime and climate, atmospheric emissions and
92 pollution, amongst others. One such ET product currently available is provided from the
93 geostationary orbit Spinning Enhanced Visible Infra-Red Imager (SEVIRI) of the Meteostat
94 Second Generation (MSG) satellite. In this product, ET is estimated operationally every 30' from
95 the SEVIRI radiometer, whereas a daily ET flux operational product is also generated with a lag
96 time of one day at a spatial resolution of 3.1 km at the sub-satellite point. These two products
97 are provided for the full disk divided in four sub regions (Europe, North Africa, South Africa and
98 South America) through the LSA-SAF web site (see <http://landsaf.meteo.pt/>). Yet, to our
99 knowledge, very few validation studies have been concerned with establishing the accuracy of
100 the SEVIRI ET instantaneous operational product, particularly at a continental scale. Such
101 studies have so far been focused primarily on performing either direct comparisons against
102 corresponding *in-situ* measurements acquired concurrently (Hu *et al.*, 2015; Petropoulos *et al.*,
103 2015b), or others based on performing inter-comparison studies against other operational
104 products or model outputs (Fensholt *et al.*, 2011; Ghilain *et al.*, 2011). Indeed, thus far only a few
105 other validations of SEVIRI ET product have been published and these have focused on
106 evaluating the product accuracy on a continental scale (Sepulcre-Canto *et al.*, 2014). As such,
107 there is an urgent need for more validation studies on this product.

108 In this context, the aim of this study has been to evaluate the accuracy of the SEVIRI ET
109 operational product at a range of European ecosystems for 2 complete years of analysis. This is
110 achieved through examining the agreement between these estimates and rates of ET measured
111 at a range of CarboEurope flux tower sites with respect to (i) different land-use and land cover
112 types commonly found in Europe; (ii) seasonality and (iii) experimental site(s) heterogeneity as
113 expressed by the Fractional Vegetation Cover (FVC).

114

115 **2. EXPERIMENTAL SET UP**

116 **2.1 Datasets**

117 *2.1.1 MSG-2 SEVIRI ET Estimates*

118 A series of operational products from SEVIRI are provided by EUMETSAT at no cost, distributed
119 by the Satellite Application Facility (SAF) on Land Surface Analysis (LSA)
120 (<http://landsaf.meteo.pt/>). For the purposes of the study, the SEVIRI instantaneous ET product
121 (MET) was acquired for the Euro region of the Meteostat disk. The method developed by LSA-SAF
122 allows estimation of both the instantaneous and daily total ET by the MSG SEVIRI radiometer. It
123 follows a physically-based approach and can be described as a simplified SVAT model modified
124 to accept EO data combined with data from other sources as forcing. The SVAT model employed
125 is essentially a simplified version of the SVAT model TESSEL (Tiled ECMWF Surface Scheme for
126 Exchange Processes over Land; (Viterbo and Beljaars, 1995), which computes land surface
127 processes taking both EO and atmospheric parameters as inputs. The algorithm is then adapted
128 to accept real-time data from meteorological satellites as forcing (Gellens-Meulenberghs *et al.*,
129 2007). The main forcing to the model comes from the remote sensing inputs including the daily
130 albedo (Geiger *et al.*, 2008a) and half-hourly short-wave (Geiger *et al.*, 2008b) and long-wave
131 fluxes (Ineichen *et al.*, 2009). To provide ET with a limited amount of missing values, a gap filling
132 procedure is also adopted in the operational algorithm. The daily ET operational product is
133 derived by temporal integration of instantaneous ET operational product values. The integration

134 limits correspond to the first (theoretically at 00:30 UTC) and last (theoretically at 24:00 UTC)
135 existing slots for a given day, and the integration step is 30'. A detailed description of the SEVIRI
136 operational ET estimation algorithm is available in Ghilain *et al.*, (2011). The retrieval accuracy
137 of ET is generally claimed to be 25% if ET is greater than 0.4 mm h⁻¹ and 0.1 mm h⁻¹ in any other
138 case (Ghilain *et al.*, 2011). The MET product contains instantaneous values of ET (in mm h⁻¹) plus
139 an associated quality flag (MSG-2 ET Product ATBD, 2008).

140 In addition, the SEVIRI FVC product was also acquired to facilitate the analysis of site
141 heterogeneity on ET retrieval accuracy. This product is generated daily at the full spatial
142 resolution of the MSG/SEVIRI instrument (3 km). It is computed using three short-wave
143 channels as inputs (VIS 0.6µm, NIR 0.8µm, SWIR 1.6µm) and a parametric Bi-directional
144 Reflectance Distribution Function (BRDF) model. In the product, FVC is delivered daily and is
145 expressed as percentage corrected from uncertainty derived of the view/sun angles and also the
146 anisotropy effects of surface reflectance in the SEVIRI image. The FVC product includes routine
147 quality check and error estimates. For each day and geographical region, the FVC product, its
148 error estimate and the processing flag were acquired in Hierarchical Data Format (HDF5) and
149 HDF5 file attributes. In our study, the SEVIRI FVC product was downloaded for the Euro region
150 of the Meteosat disk for both 2010 and 2011. All SEVIRI data was obtained free of charge
151 through the LSA-SAF web site (see <http://landsaf.meteo.pt/>).

152
153

154 2.1.2 Study Sites: In-situ ET Measurements

155 *In-situ* ET measurements for a total of 7 flux experimental sites of the CarboEurope network
156 (Baldocchi, 2003) were utilised in this study. CarboEurope is part of FLUXNET, the largest global
157 "network of regional networks" to coordinate regional and global analysis of
158 micrometeorological fluxes and ancillary parameters. The flux tower sites of the individual
159 networks utilise the same eddy covariance method to measure the exchanges of carbon dioxide
160 (CO₂), water vapour, and energy between terrestrial ecosystems and the atmosphere to a good
161 level of standardisation. This enables uniform measurement comparisons between sites and
162 datasets. ET is measured as a core parameter at half-hourly intervals using the eddy covariance
163 system. In our study, *in-situ* data for the complete years 2010 and 2011 were acquired from 7
164 CarboEurope sites of varying environmental and ecosystem conditions. These sites included 5
165 situated within a Mediterranean environment (Spain and Italy) and 2 others located in
166 temperate climate zones (France and UK), representative of open shrubland, grassland,
167 evergreen needle-leaf forest and cropland land cover types. In this study sites were only selected
168 where continuous long term datasets are available for use. Further, during the selection of sites
169 weather conditions are also a deciding factor when using the Visible/Infrared satellite
170 measurements. Sometime data are available but due to cloudy conditions either there is high
171 noise in the datasets or not available at all over the installed Fluxnet sites. Other important
172 factors during the selection of sites are homogeneity in the land cover type. To avoid any mixed
173 pixel effects on the overall performance, satellite pixels are chosen over the Fluxnet tower
174 having the large homogenous land cover. In addition, the sites proposed are a complementary
175 selection compared to other validation studies of the same product. Site names and their main
176 characteristics are listed in **Table 1**. All *in-situ* data were obtained from the CarboEurope
177 website (<http://gaia.agraria.unitus.it/>) and where possible, verified by the site manager.

178

179 2.2 Methods

180 The acquired ET product images were re-projected from Normalized Geostationary Projection
181 (NGP) to a regular latitude/longitude grid and tailored from the full disk image to the study
182 region (34°-45°N, 11°W-5°E). Each image was subsequently clipped into the separate European
183 countries in which our experimental sites were located. Periods for which more than 10 % of
184 each of the half-hour SEVIRI estimated ET (granules) was missing from a “site-day” were
185 omitted from the comparisons. The data were further refined by excluding granules with
186 negative values from the dataset. These values corresponded to flags or no-data values which
187 were inappropriate for use in assessing the agreement between both datasets. In addition, a
188 scaling factor was applied to each MET 30’ product to derive the actual ET value (MSG-2 ET
189 Product ATBD, 2008). Subsequently, the pre-processed *in-situ* ET values that corresponded to
190 the date/time of the satellite overpass were extracted (Excel MacroVBA), and assigned to point
191 shapefiles of the test sites, where there was one shapefile per country (tabular join in ArcMap
192 10.1). These shapefiles were overlain on the pre-processed SEVIRI images in the BEAM VISAT +
193 SMOS toolbox. Using the BEAM correlation tool, the *in-situ* ET was matched against the SEVIRI
194 ET of the pixel containing the site point. These pixels were then extracted to Microsoft Excel for
195 further analysis and comparisons against the *in-situ* data.

196

197 2.3 Statistical Analysis

198 Agreement between the ET SEVIRI predictions and the corresponding *in-situ* data was evaluated
199 based on direct point by point comparisons. Several statistical performance assessment metrics
200 were used to evaluate the agreement between the compared datasets. These included the Root
201 Mean Square Difference (RMSD), the Pearson’s Correlation Coefficient (r) (including the Slope
202 and Intercept of the regression equation), the Mean Bias Error (MBE) or Bias (*in-situ* minus
203 estimated), and the Mean Standard Deviation (MSD) or Scatter. A robust regression was
204 computed using iterative re-weighted least squares (Street *et al.*, 1988), which is influenced less
205 by outliers than the ordinary least-squares fit (Entekhabi *et al.*, 2010). These statistical metrics
206 have been prominently used in analogous validation experiments of relevant operational
207 products validation studies (e.g. LSA-SAF Validation Report Evapotranspiration Products, 2010).

208 Additional analyses were performed exploring the agreement between the satellite-derived and
209 *in-situ* ET as a function of land cover type, seasonality and surface heterogeneity (expressed as
210 FVC percentage derived from the SEVIRI FVC product). For the analysis by land cover type,
211 agreement was evaluated for 7 sites inclusive of 4 different land cover types: ES_Agu and ES_Lju
212 – open shrubland, IT_Ren – Evergreen Needle-Leaf Forest, IT_Mbo and UK_Ebu – grasslands,
213 IT_Cas and FR_Mau – croplands. Similarly, agreement was also evaluated for the 4 seasons,
214 spring (Mar-May), summer (Jun-Aug), autumn (Sep-Nov) and winter (Dec-Feb), and analysed
215 separately for FVC ranges with different percentage coverage thresholds: 0-24, 25-49, 50-74 and
216 75-100. Direct point-by-point comparisons were performed at every *in-situ* station to evaluate
217 the statistical agreement for each threshold. Analysis was performed for each scenario
218 independently for both 2010 and 2011, and also for both years combined into a single dataset.

219

220 3. RESULTS

221 This study has been concerned with the verification of the operational retrieval of satellite-
222 derived ET estimates from the MSG SEVIRI sensor. **Table 2** illustrates the key results from the
223 comparison between the satellite-derived ET estimates and the corresponding *in-situ* observed
224 for all days of analysis per experimental site. In **Figure 1**, examples of spatial maps of ET derived
225 from the SEVIRI operational product on the 6th of August 2011 for Spain at two different times of
226 day are shown (7a.m. UTC/11a.m. UTC). A qualitative comparison of the spatial distribution of

227 ET in comparison to the FVC indicates a good agreement in the spatial patterns between both
228 the SEVIRI FVC and MET products, highlighting a key link between ET spatial distribution and
229 other biophysical parameters. It can be observed from **Figure 1** that the areas of maximum ET
230 estimation (which range between 0.093 and 0.523 mm h⁻¹ dependent on time of day) can be seen
231 in northern Spain, which clearly correspond to the areas of maximum FVC (up to 100%) for the
232 same date (FVC is provided as a daily product). The larger area to the south and south east
233 exhibited low to very low (near zero) ET, which again correlate with areas of low FVC. There is
234 also a clear trend in the dynamic rates of ET at different times throughout the day, underlining
235 the capability of the operational product to capture the temporal variability of ET. ET rates are at
236 their lowest point during the early morning, increasing to their maximum at midday and then
237 decreasing yet again in the early afternoon, showing a positive correlation with amount of
238 incoming solar radiation at the surface.

239 Despite the variability in accuracy found in different land covers, seasons and using different
240 FVC thresholds (sections 3.1, 3.2, 3.3), in absolute terms, a good agreement was found between
241 the two datasets, with a correlation between the point predicted ET resulting in an r of 0.709.
242 The SEVIRI MET estimates exhibited a minor overestimation of the observed with a mean
243 positive bias of 0.001 mm h⁻¹. The mean scatter of 0.065 mm h⁻¹, although a significant increase
244 on the bias results, indicated a reliable estimation of the in-situ data by the operational product.
245 Evidently, the mean RMSD of 0.065 mm h⁻¹ in the estimation of ET when all days were
246 considered was within the accepted accuracy range for the operational retrieval of ET (retrieval
247 within ~25% of in-situ if ET is greater than 0.4 mm h⁻¹ (LSA-SAF, 2010; (Ghilain *et al.*, 2011)).
248 These findings are also well-aligned to previous analogous validation studies of the SEVIRI MET
249 product (e.g. (Ghilain *et al.*, 2011)(Petropoulos *et al.*, 2015b).

250 3.1 Land use and land cover comparisons

251 **Table 2** summarises the comparisons of predicted and observed rates of ET on the seven
252 experimental sites of varying land use and land cover in 2010 and 2011. In general, when data
253 for both years combined are plotted for the individual sites, it is clear that the grassland and
254 cropland sites (IT_Mbo/IT_Cas/Fr_Mau/UK_Ebu) exhibited the closest agreement of all land
255 cover types (r from 0.705 to 0.759). However, notably, this is not reflected in the error metrics
256 (**Table 2**) where both the shrubland sites (ES_Agu/ES_Lju) returned the lowest RMSD and MAE
257 of all sites, between 0.035-0.044 mm h⁻¹ and between 0.021-0.025 mm h⁻¹ respectively. In
258 comparison, the agreement over the grassland and cropland sites resulted in much higher error
259 ranges (UK_Ebu being the only exception). The error results are also mirrored in the bias and
260 scatter results, where the three sites of lowest RMSD (ES_Agu/ES_Lju/UK_Ebu) exhibited a
261 decrease in scatter and bias of ~50% in comparison to all other sites. Evidently, the RMSD is
262 derived predominantly from the scatter and not the bias for all sites. Interestingly, the poorest
263 performing site when both years were combined was the IT_Ren Evergreen Needleleaf Forest
264 site (RMSD of 0.093 mm h⁻¹), suggesting that the taller and/or denser vegetation cover may have
265 detrimental implications for the operational products retrieval accuracy.

266 When sites were analysed per year, similar trends were clearly evident (**Table 2**). In 2010, the
267 bias is low for all land use and land cover types (< 0.030 mm h⁻¹) and this is also the case in 2011
268 where the maximum bias is 0.024 mm h⁻¹. The lowest errors are seen in sites with short or low
269 vegetation cover and areas which contain bare ground i.e. the shrublands of ES_Agu and ES_Lju,
270 and the grassland of UK_Ebu where the RMSD are all below 0.04 mm h⁻¹. These sites also show
271 the lowest bias (all within 0.007 mm h⁻¹ in 2010, with variation by site) and the lowest scatter
272 which is also less than 0.04 mm h⁻¹. The highest correlations between predicted and observed ET

273 rates are seen in the grasslands sites of UK_Ebu and IT_Mbo ($r > 0.700$). These results are
274 generally mirrored in the results for 2011, with some differences. For example, although bias
275 and errors are still low, they are greater than in 2010 than in 2010 for the ES_Agu, ES_Lju and
276 UK_Ebu sites. The correlation in 2011 for IT_Mbo is lower than that recorded for 2010 at 0.706,
277 but the correlation for UK_Ebu continues to be high. In overall, when results are stratified by
278 year, trends in product accuracy dependent on land cover are clearly evident. Furthermore,
279 error for all sites is predominantly the result of scatter rather than the bias.

280 *3.2 Seasonality*

281 The temporal trends between in-situ and predicted ET from SEVIRI for different seasons during
282 2010 and 2011 are shown in **Figure 2a-b** for few selected sites. In general, comparisons
283 between the in-situ and SEVIRI ET time series exhibit a high temporal variability with seasons
284 and depicting a strong seasonal cycle. Generally, ET values are highly responsive with the
285 seasonality indicated by marked fluctuations over the entire period with rapid and sharp
286 responses, even to small changes in weather. The pattern shows that months from June-August
287 (summer) are drier with ET values peaking during these months. Further, ET started to decrease
288 during the autumn (September to November) with its lowest values during December to
289 February (winter). Rising temperatures in Europe from spring to summer are reflected in a
290 gradual rise in ET during this period. From the results summarised in those figures it is evident
291 that in summer, typically, very high ET values were found, while during the winters a decline in
292 ET values are recorded. Increasing temperatures and high evaporation through the summer
293 period lead to a progressive drying of the soil and therefore decreasing ET values. Some dips in
294 the ET values during the summer can be attributed to some short-duration storms. Generally
295 winter is the relatively wettest period during the analysis, because of occurrence of some
296 precipitation events, further solar radiation and temperature are also low during the winters
297 leading to decreases in ET rates during winter months.

298 **Table 3** summarises the comparisons between winter, spring, summer and autumn ET rates for
299 all sites together in 2010 and 2011. **Figure 3** shows the agreement between predicted and
300 observed ET rates for the different seasons separately for 2011 and 2012. In common with the
301 results for land cover and land use type, the bias is very low (all within 0.020 mm h^{-1}), as are the
302 scatter and RMSD (all less than 0.100 mm h^{-1}). RMSD seems to be at its highest in spring and
303 summer. The main pattern that can be seen in these results is that the correlation between
304 predicted and observed rates of evaporation seems to be strongest during the summer and
305 autumn. This is the case when both years are taken together, and when the two years are taken
306 apart (e.g. the correlation coefficient is 0.714 and 0.687 in summer and autumn respectively
307 when both years are taken together, 0.731 and 0.706, respectively in 2010 and 0.707 and 0.685,
308 respectively in 2011). The weakest correlations are seen in winter, in 2010 and 2011 and when
309 both years are taken together. The correlation patterns which are observed are strengthening of
310 the correlation as the year progresses from winter through spring, summer and on to autumn,
311 possibly reflecting the increasing areal extent of homogenous vegetation cover from winter to
312 spring and summer, and a slight loss as that vegetation cover begins to be lost during the
313 autumn. Interestingly, the error statistics, in contrast to the correlation results, exhibit the
314 adverse trend, with highest RMSD and MAD prevalent during the spring and summer months for
315 both years separately and also for the 2 years combined. Similarly to the land cover results,
316 error was predominantly the result of high scatter and not the bias prediction.

317

318 *3.3 Fractional Vegetation Cover*

319 **Table 4** shows the comparison of ET rate statistics for all sites in 2010 and 2011 with four
320 different thresholds of FVC (0-0.24/0.25-0.49/0.50-0.74/0.75-1) ranging from 0 to 1, and **Table**
321 **5** summarises these data for both years combined and for all experimental sites. Also **Figure 4**
322 shows the agreement between the predicted ET and in-situ for different FVC ranges. By
323 investigating the agreement between the two datasets within varying FVC thresholds, it is possible
324 to analyse the influence of site or land cover homogeneity on the accuracy of the ET operational
325 product retrieval. When data for all sites and years were combined, bias was once again low for
326 all FVC thresholds (all thresholds within 0.020 mm h⁻¹). Scatter and RMSD results (**Table 5**)
327 were low for 3 out of the 4 bands when both years of data were combined, <0.67 mm h⁻¹ and
328 <0.69 mm h⁻¹ for scatter and RMSD respectively, with the 0.50-0.74 FVC threshold being the only
329 exception, resulting in high scatter and RMSD above 0.1 mm h⁻¹. Although both the 0.25-0.49 and
330 0.75-1 thresholds exhibited lower error in comparison to the 0.50-0.74 threshold, they were still
331 markedly higher compared to the RMSD for the lowest FVC threshold (0-0.24) (0.042 mm h⁻¹).
332 Overall, the error statistics results suggested a positive trend between RMSD and FVC
333 percentage i.e. as FVC increases the RMSD also increases in correlation.

334 The correlation between predicted and observed rates shows a generally strengthening trend
335 moving from the low FVC thresholds to the highest (**Figure 4**). For example, in 2011 the
336 correlation coefficient increased from 0.430 in the 0-0.24 band to 0.674 in the 0.25-0.49 band to
337 0.690 in the 0.50-0.74 band and to 0.771 in the 0.75-1 band. This pattern was mirrored when
338 both years were taken together. The only outlier to this pattern was a weaker correlation in the
339 0.25-0.49 band in 2010 than was observed in the 0-0.25 band. This increase in correlation could
340 again be related to the increasing homogeneity of the land cover as FVC increases, thus
341 decreasing the spatial variability in land cover and ET rates.

342 More variability is apparent, however, when the sites are treated separately (**Table 4**). At sites
343 where there is more than one FVC threshold (ES_Agu/IT_Ren/IT_Mbo/UK_Ebu) the pattern is
344 less clear. At ES_Agu, the correlation strengthens as FVC increases in 2010, but decreases in
345 2011. At IT_Ren, a steady increase in the correlation coefficient is seen in 2010, but a decrease is
346 seen between the 0.5-0.74 and the 0.75-1 FVC thresholds in 2011. At UK_Ebu, the correlation
347 strengthens in 2011, but weakens between the 0.5-0.74 and the 0.75-1 FVC thresholds in 2011.
348 At IT_Mbo an increase in the correlation coefficient is seen in both years. Mirroring the results
349 seen for the land use and land cover analysis, the strongest correlations (generally greater than
350 0.75) are seen in the Grassland/Cereal Crops of IT_Mbo, UK_Ebu and FR_Mau, where the
351 homogeneity of vegetation species, extent and crown elevation is greater and thus where the
352 rates of ET are more uniform.

353

354 **4. DISCUSSION**

355 This study represents a systematic and robust evaluation of the SEVIRI ET operational product
356 at selected ecosystems in Europe for the period of 2010-2011. The effect of varying land cover,
357 landscape homogeneity (percentage of FVC) and seasonality on the accuracy of the ET retrieval
358 algorithm is analysed, allowing a more robust and comprehensive evaluation of the performance
359 of the operational product. Overall, findings of the study were similar to previous validations of
360 the SEVIRI ET product (e.g. Ghilain *et al.*, 2011; Gellens-Meulenberghs *et al.*, 2012; Petropoulos *et*
361 *al.*, 2015b). The agreement between the ET predicted from SEVIRI and the CarboEurope *in-situ*
362 measurement returned a high correlation coefficient ($r = 0.709$), highlighting a strong linear
363 relationship between the two datasets and suggesting that the satellite product showed good

364 ability to estimate actual ET measurements. The low error metrics represented by an RMSD and
365 MAE of 0.065 mm h⁻¹ and 0.037 mm h⁻¹ respectively, indicated that the results of the study met
366 the quality criterion adopted to assess the quality of the results as suggested by the EUMETSAT
367 operational product development team. These criterion were the following: error within 25% of
368 the *in-situ* if ET is greater than 0.4 mm h⁻¹ and error within 0.1 mm h⁻¹ of the *in-situ* if ET is less
369 0.4 mm h⁻¹ (Ghilain *et al.*, 2011). These results underline the potential applicability of the SEVIRI
370 MET product for operational implementation over Europe.

371 When results were stratified by land cover type, a clear inter-site variability in retrieval accuracy
372 was evident. The open shrubland site of ES_Agu, Spain returned the lowest error of all sites
373 (RMSD of 0.035 mm h⁻¹) with ES_Lju also performing well (RMSD of 0.044 mm h⁻¹). The SEVIRI
374 MET product was able to reliably estimate ET rates over the open shrubland land cover types,
375 particularly in the Mediterranean region. This could be due to a more consistent land cover
376 extent and type throughout the year, compared to the varying nature of cropland, for example.
377 Furthermore, the performance degradation at ES_Agu between 2010 and 2011 might be due to a
378 change of input data characteristics of the operational product, particularly from the ECMWF
379 forecasts of superficial soil moisture (change of parameterization, with a new operational cycle
380 end of 2010), in the implementation of the ET algorithm. The highest error (RMSD of 0.1 mm h⁻¹)
381 bias (0.028 mm h⁻¹) and scatter (0.096 mm h⁻¹) were seen for the cropland site of IT_Cas in Italy,
382 with the other cropland site of FR_Mau in France exhibiting similar high error statistics. This
383 may be due to sub-annual, temporal changes in land use and/or land cover depending on the
384 growing season and different agricultural practices that reduce the type and height of
385 vegetation. The high error, scatter and bias at IT_Mbo, and high error at IT_Ren, Italy are more
386 difficult to explain given that they are grassland and evergreen forests sites, respectively, and
387 would not be subject to as many changes, especially in terms of agricultural practices. A possible
388 reason for this would be the more frequent occurrence of seasonal snow cover at these sites,
389 leading to a greater annual variability in land surface characteristics than suggested by
390 vegetation type alone. In fact, the IT_MBo and IT_Ren are both situated in a mountainous
391 environment where there is a lot of uncertainty potentially introduced to the ET retrievals due
392 to fragmentation of landscape between forests and alpine pastures, and as discussed, due to
393 snow cover. This can lead to uncertainty in the remote sensing signal and in the accuracy of the
394 numerical weather forecasts used as input in such regions, resulting to a significant impact on
395 the remotely sensed ET retrievals.

396 Previous examinations of the performance of the SEVIRI MET algorithm over different land
397 cover types in Europe have also returned comparable results and observations to those reported
398 in this study. Ghilain *et al.*, (2012) performed a validation of the SEVIRI MET product through
399 direct comparisons with *in-situ* data over four land cover types in Europe. Both the grassland
400 and evergreen forest sites returned high errors comparable to this study. Similarly, Ghilain *et al.*,
401 (2011) evaluated the performance of the operational products algorithm over six European
402 sites. The algorithm again performed poorly over grassland sites (RMSD ranging between 0.07
403 to 1 mm h⁻¹). More recently, Petropoulos *et al.*, (2015b), evaluated the SEVIRI ET estimates
404 against *in-situ* data for 9 sites from the CarboEurope network. A clear correlation was also
405 evident between the performance of the algorithm dependent on land cover type between the
406 result presented herein and those of Petropoulos *et al.*, (2015b), with open shrubland (0.049
407 mm h⁻¹) sites outperforming the grassland (RMSD of 0.072 mm h⁻¹) and evergreen forest sites
408 (RMSD of 0.152 mm h⁻¹). Notably, all authors reported an overestimation of the *in-situ* data by
409 the MET product in a significant majority of the comparisons, which is something also found in
410 this study.

411 Although the results presented herein underline the significant potential of the SEVIRI ET
412 operational product for the accurate estimation of ET, a number of possible sources of error for
413 the satellite-based daily ET estimates and limitations on the flux tower measurements exist. In
414 this study, the satellite data are assumed to represent the average of a grid cell corresponding to
415 the station fetch used for validation. This assumption can be problematic, as a large spatial
416 discrepancy exists between the coarser satellite-based ET retrievals (3 km spatial resolution),
417 and the flux tower measurements (a fetch in the order of meters). In sites of diverse land cover
418 conditions (fragmented, different vegetation types, areas of bare soil), different ET values are
419 prevalent at different spatial scales. Thus if a remotely sensed footprint includes heterogeneous
420 and/or rough terrain, eddy formation can be highly variable and may not be consistent with that
421 of the flux tower fetch (Marshall *et al.*, 2013). Furthermore, since the majority of flux towers are
422 located in close proximity to vegetated areas, they tend to give higher ET measurements than
423 the spatially averaged satellite values, particularly so in more fragmented landscapes (Sun *et al.*,
424 2012). This discrepancy was evident when analysing the correlation between the satellite
425 estimates and the *in-situ* data in the study herein, where a positive correlation was exhibited
426 between the percentage of FVC and R. These results suggest that the higher the FVC (i.e. the
427 more homogenous the site), the more representative the ET point measurements were of the
428 SEVIRI MET pixel. A possible solution to overcome the issue of spatial discrepancy and
429 representativeness between the datasets would be to evaluate the satellite-based estimates
430 using several flux towers within a satellite grid cell/footprint, each tower representing the
431 various land cover types and taking a weighted average to compare to the coarser remotely
432 sensed estimate (Marshall *et al.*, 2013). Limitations are also evident concerning the “ground
433 truth” data used to validate the operational product. Measured surface-atmosphere fluxes of
434 energy (H and LE) and CO₂ by the eddy covariance method represents the “true” flux plus or
435 minus potential random and systematic measurement errors (Wilson *et al.*, 2002; Petropoulos *et*
436 *al.*, 2013). Generally, the verification or validation of fluxes by the eddy covariance utilises the
437 energy balance closure (EBC) approach. A lack of EBC with the eddy correlation technique, as
438 used in FLUXNET, has been shown to lead to uncertainty on fluxes measurement up to ~20%,
439 which could potentially be translated to a lack of accuracy when compared against satellite
440 retrievals (Falge *et al.*, 2002; Wilson *et al.*, 2002) . EBC may also ignore any biases in the half-
441 hourly data, where for example, there is trend for the eddy covariance system to overestimate
442 positive fluxes during the daytime and underestimate negative fluxes at night (Mahrt, 1998).

443

444 5. CONCLUSIONS

445 The aim of this study was to perform an extensive and systematic evaluation of the operationally
446 distributed SEVIRI evapotranspiration (ET) product at 7 selected European sites belonging to
447 the CarboEurope ground monitoring network, representative of a variety of land cover
448 characteristics. To our knowledge, our study is one of the few published so far that provides
449 such a comprehensive evaluation of this operational product, looking at evaluating the product
450 accuracy from different perspectives.

451 Overall, the point by point comparisons between the satellite and *in-situ* ET for the combined
452 dataset of all days of analysis resulted in a close agreement (r of 0.709) and a low error exhibited
453 by the model (RMSD of 0.065 mm h⁻¹). Those findings were comparable to similar validation
454 studies. A clear inter-site variability in retrieval accuracy was evident when results were
455 stratified by land cover type. With regards to the seasonal differences in SEVIRI MET retrieval
456 performance, RMSD was at its highest in spring and summer, whereas the correlations between

457 predicted and observed rates of evaporation were strongest during the summer and autumn.
458 Results suggest that the higher the FVC (i.e. the more homogenous the site), the more
459 representative the ET point measurements were of the SEVIRI MET pixel, overcoming issues
460 related to spatial discrepancy between the datasets.

461 An update of the algorithm (version 2) is foreseen to release the ET products in 2016, with an
462 expected improvement of the quality and the stability over dry areas thanks to the assimilation
463 of more SEVIRI products, like land surface temperature and vegetation related characteristics .
464 Studies such as this are important steps in the validation of operational satellite products and
465 are vital for the future development of SEVIRI's operational capacity on a global scale. The
466 identification of strengths and weaknesses of the current operational products by means of such
467 studies is a driver of new capabilities developments.

468 **Acknowledgments**

469 Implementation of this work has been supported by the FP7-People project TRANSFORM-EO
470 (project reference number 334533) as well as the High Performance Computing Facilities of
471 Wales (HPCW) project PREMIER-EO. Dr Petropoulos as the PI of both project wishes to thank
472 both funding bodies for supporting the implementation of this research study. Authors are also
473 grateful to the CarboEurope site managers and to the SEVIRI LSA-SAF team for the provision of
474 the data used in this study. Finally authors wish to thank the reviewers for their valuable
475 comments which helped improving the manuscript.

476

477 **References:**

- 478 Baldocchi, D.D., 2003. Assessing the eddy covariance technique for evaluating carbon dioxide
479 exchange rates of ecosystems: past, present and future. *Global Change Biology* 9, 479-492.
- 480 Buytaert, W., Céleri, R., De Bièvre, B., Cisneros, F., Wyseure, G., Deckers, J., Hofstede, R., 2006.
481 Human impact on the hydrology of the Andean páramos. *Earth-Science Reviews* 79, 53-72.
- 482 Cruz-Blanco, M., Lorite, I., Santos, C., 2014. An innovative remote sensing based reference
483 evapotranspiration method to support irrigation water management under semi-arid
484 conditions. *Agricultural Water Management* 131, 135-145.
- 485 Entekhabi, D., Reichle, R.H., Koster, R.D., Crow, W.T., 2010. Performance metrics for soil
486 moisture retrievals and application requirements. *Journal of Hydrometeorology* 11, 832-
487 840.
- 488 Falge, E., Baldocchi, D., Tenhunen, J., Aubinet, M., Bakwin, P., Berbigier, P., Bernhofer, C., Burba,
489 G., Clement, R., Davis, K.J., 2002. Seasonality of ecosystem respiration and gross primary
490 production as derived from FLUXNET measurements. *Agricultural and Forest Meteorology*
491 113, 53-74.
- 492 Fensholt, R., Anyamba, A., Huber, S., Proud, S.R., Tucker, C.J., Small, J., Pak, E., Rasmussen, M.O.,
493 Sandholt, I., Shisanya, C., 2011. Analysing the advantages of high temporal resolution
494 geostationary MSG SEVIRI data compared to Polar Operational Environmental Satellite data
495 for land surface monitoring in Africa. *International Journal of Applied Earth Observation*
496 and *Geoinformation* 13, 721-729.
- 497 Geiger, B., Carrer, D., Franchistéguy, L., Roujean, J.-L., Meurey, C., 2008a. Land surface albedo
498 derived on a daily basis from Meteosat second generation observations. *Geoscience and*
499 *Remote Sensing, IEEE Transactions on* 46, 3841-3856.
- 500 Geiger, B., Meurey, C., Lajas, D., Franchistéguy, L., Carrer, D., Roujean, J.L., 2008b. Near real-time
501 provision of downwelling shortwave radiation estimates derived from satellite
502 observations. *Meteorological Applications* 15, 411-420.
- 503 Gellens-Meulenberghs, F., Arboleda, A., Ghailain, N., 2007. Towards a continuous monitoring of
504 evapotranspiration based on MSG data. *IAHS PUBLICATION* 316, 228.

505 Gellens-Meulenberghs, F., Ghilain, N., Arboleda, A., 2012. Land surface evapotranspiration as
506 seen from Meteosat Second Generation Satellites: LSA-SAF developments and perspectives.
507 Geoscience and Remote Sensing Symposium (IGARSS), 2012 IEEE International. IEEE, pp.
508 1018-1021.

509 Ghilain, N., Arboleda, A., Gellens-Meulenberghs, F., 2011. Evapotranspiration modelling at large
510 scale using near-real time MSG SEVIRI derived data. *Hydrology and Earth System Sciences*
511 15, 771-786.

512 Ghilain, N., Arboleda, A., Sepulcre-Cantò, G., Batelaan, O., Ardö, J., Gellens-Meulenberghs, F.,
513 2012. Improving evapotranspiration in a land surface model using biophysical variables
514 derived from MSG/SEVIRI satellite. *Hydrology and Earth System Sciences* 16, 2567-2583.

515 Ghilain, N., De Roo, F., Gellens-Meulenberghs, F., 2014. Evapotranspiration monitoring with
516 Meteosat Second Generation satellites: improvement opportunities from moderate spatial
517 resolution satellites for vegetation. *International Journal of Remote Sensing* 35, 2654-2670.

518 Hu, G., Jia, L., Menenti, M., 2015. Comparison of MOD16 and LSA-SAF MSG evapotranspiration
519 products over Europe for 2011. *Remote Sensing of Environment* 156, 510-526.

520 Ineichen, P., Barroso, C.S., Geiger, B., Hollmann, R., Marsouin, A., Mueller, R., 2009. Satellite
521 Application Facilities irradiance products: hourly time step comparison and validation over
522 Europe. *International Journal of Remote Sensing* 30, 5549-5571.

523 Ireland, G., Petropoulos, G.P., Carlson, T.N., Purdy, S., 2015. Addressing the ability of a land
524 biosphere model to predict key biophysical vegetation characterisation parameters with
525 Global Sensitivity Analysis. *Environmental Modelling & Software* 65, 94-107.

526 Jia, Z., Liu, S., Xu, Z., 2010. Validation of remotely sensed evapotranspiration: a case study.
527 Geoscience and Remote Sensing Symposium (IGARSS), 2010 IEEE International. IEEE, pp.
528 2119-2122.

529 Jones, J.A.A., 2014. *Water sustainability: a global perspective*. Routledge.

530 Jung, M., Reichstein, M., Ciais, P., Seneviratne, S.I., Sheffield, J., Goulden, M.L., Bonan, G., Cescatti,
531 A., Chen, J., De Jeu, R., 2010. Recent decline in the global land evapotranspiration trend due
532 to limited moisture supply. *Nature* 467, 951-954.

533 Kalivas, D., Petropoulos, G., Athanasiou, I., Kollias, V., 2013. An intercomparison of burnt area
534 estimates derived from key operational products: the Greek wildland fires of 2005–2007.
535 *Nonlinear Processes in Geophysics* 20, 397-409.

536 Legesse, D., Vallet-Coulomb, C., Gasse, F., 2003. Hydrological response of a catchment to climate
537 and land use changes in Tropical Africa: case study South Central Ethiopia. *Journal of*
538 *Hydrology* 275, 67-85.

539 Mahrt, L., 1998. Nocturnal boundary-layer regimes. *Boundary-layer meteorology* 88, 255-278.

540 Marshall, M., Tu, K., Funk, C., Michaelsen, J., Williams, P., Williams, C., Ardö, J., Boucher, M.,
541 Cappelaere, B., Grandcourt, A.d., 2013. Improving operational land surface model canopy
542 evapotranspiration in Africa using a direct remote sensing approach. *Hydrology and Earth*
543 *System Sciences* 17, 1079-1091.

544 Mueller, B., Seneviratne, S., Jimenez, C., Corti, T., Hirschi, M., Balsamo, G., Ciais, P., Dirmeyer, P.,
545 Fisher, J., Guo, Z., 2011. Evaluation of global observations-based evapotranspiration datasets
546 and IPCC AR4 simulations. *Geophysical research letters* 38.

547 Petropoulos, G., Ireland, G., Cass, A., Srivastava, P., 2015a. Performance Assessment of the
548 SEVIRI Evapotranspiration Operational Product: Results Over Diverse Mediterranean
549 Ecosystems. *IEEE Sensors*. DOI:10.1109/jsen.2015.2390031.

550 Petropoulos, G.P., Carlson, T.N., Griffiths, H.M., 2013. Turbulent Fluxes of Heat and Moisture at
551 the Earth's Land Surface: Importance, Controlling Parameters, and Conventional
552 Measurement Techniques. *Remote Sensing of Energy Fluxes and Soil Moisture Content*, 1.

553 Petropoulos, G.P., Ireland, G., Cass, A., Srivastava, P.K., 2015b. Performance assessment of the
554 SEVIRI evapotranspiration operational product: results over diverse mediterranean
555 ecosystems. *Sensors Journal*, IEEE 15, 3412-3423.

556 Remesan, R., Holman, I.P., 2015. Effect of baseline meteorological data selection on
557 hydrological modelling of climate change scenarios. *Journal of Hydrology* 528, 631-642.

558 Sepulcre-Canto, G., Vogt, J., Arboleda, A., Antofie, T., 2014. Assessment of the EUMETSAT LSA-
559 SAF evapotranspiration product for drought monitoring in Europe. *International Journal of*
560 *Applied Earth Observation and Geoinformation* 30, 190-202.

561 Smolders, A., Hudson-Edwards, K., Van der Velde, G., Roelofs, J., 2004. Controls on water
562 chemistry of the Pilcomayo river (Bolivia, South-America). *Applied Geochemistry* 19, 1745-
563 1758.

564 Srinivasan, V., Thompson, S., Madhyastha, K., Penny, G., Jeremiah, K., Lele, S., 2015. Why is the
565 Arkavathy River drying? A multiple hypothesis approach in a data scarce region. *Hydrology*
566 *and Earth System Sciences Discussions* 12, 25-66.

567 Srivastava, P.K., Han, D., Islam, T., Petropoulos, G.P., Gupta, M., Dai, Q., 2015a. Seasonal
568 evaluation of evapotranspiration fluxes from MODIS satellite and mesoscale model
569 downscaled global reanalysis datasets. *Theoretical and Applied Climatology*. DOI:
570 10.1007/s00704-015-1430-1.

571 Srivastava, P.K., Han, D., Islam, T., Petropoulos, G.P., Gupta, M., Dai, Q., 2015b. Seasonal
572 evaluation of evapotranspiration fluxes from MODIS satellite and mesoscale model
573 downscaled global reanalysis datasets. *Theoretical and Applied Climatology*, 1-13.

574 Srivastava, P.K., Han, D., Ramirez, M.A., Islam, T., 2013a. Appraisal of SMOS soil moisture at a
575 catchment scale in a temperate maritime climate. *Journal of Hydrology* 498, 292-304.

576 Srivastava, P.K., Han, D., Ramirez, M.A., Islam, T., 2013b. Machine Learning Techniques for
577 Downscaling SMOS Satellite Soil Moisture Using MODIS Land Surface Temperature for
578 Hydrological Application. *Water Resources Management* 27, 3127-3144.

579 Srivastava, P.K., Han, D., Rico-Ramirez, M.A., Islam, T., 2014. Sensitivity and uncertainty
580 analysis of mesoscale model downscaled hydro-meteorological variables for discharge
581 prediction. *Hydrological Processes* 28, 4419-4432.

582 Srivastava, P.K., Han, D., Rico-Ramirez, M.A., O'Neill, P., Islam, T., Gupta, M., Dai, Q., 2015c.
583 Performance evaluation of WRF-Noah Land surface model estimated soil moisture for
584 hydrological application: Synergistic evaluation using SMOS retrieved soil moisture. *Journal*
585 *of Hydrology* 529, Part 1, 200-212.

586 Srivastava, P.K., Han, D., Rico Ramirez, M.A., Islam, T., 2013c. Comparative assessment of
587 evapotranspiration derived from NCEP and ECMWF global datasets through Weather
588 Research and Forecasting model. *Atmospheric Science Letters* 14, 118-125.

589 Srivastava, P.K., Islam, T., Gupta, M., Petropoulos, G., Dai, Q., 2015d. WRF Dynamical
590 Downscaling and Bias Correction Schemes for NCEP Estimated Hydro-Meteorological
591 Variables. *Water Resources Management* 29, 2267-2284.

592 Street, J.O., Carroll, R.J., Ruppert, D., 1988. A note on computing robust regression estimates via
593 iteratively reweighted least squares. *The American Statistician* 42, 152-154.

594 Sun, Z., Gebremichael, M., Ardö, J., De Bruin, H., 2011. Mapping daily evapotranspiration and
595 dryness index in the East African highlands using MODIS and SEVIRI data. *Hydrology and*
596 *Earth System Sciences* 15, 163-170.

597 Sun, Z., Gebremichael, M., Ardö, J., Nickless, A., Caquet, B., Merboldh, L., Kutschi, W., 2012.
598 Estimation of daily evapotranspiration over Africa using MODIS/Terra and SEVIRI/MSG
599 data. *Atmospheric Research* 112, 35-44.

600 Taconet, O., Bernard, R., Vidal-Madjar, D., 1986. Evapotranspiration over an agricultural region
601 using a surface flux/temperature model based on NOAA-AVHRR data. *Journal of Climate and*
602 *Applied Meteorology* 25, 284-307.

603 Verstraeten, W.W., Veroustraete, F., Feyen, J., 2005. Estimating evapotranspiration of European
604 forests from NOAA-imagery at satellite overpass time: Towards an operational processing
605 chain for integrated optical and thermal sensor data products. *Remote Sensing of*
606 *Environment* 96, 256-276.

607 Viterbo, P., Beljaars, A.C., 1995. An improved land surface parameterization scheme in the
608 ECMWF model and its validation. *Journal of Climate* 8, 2716-2748.

609 Wagner, P.D., Reichenau, T.G., Kumar, S., Schneider, K., 2015. Development of a new
610 downscaling method for hydrologic assessment of climate change impacts in data scarce
611 regions and its application in the Western Ghats, India. *Regional Environmental Change* 15,
612 435-447.

613 Wang, K., Dickinson, R.E., 2012. A review of global terrestrial evapotranspiration: Observation,
614 modeling, climatology, and climatic variability. *Reviews of Geophysics* 50.
615 Wilson, K., Goldstein, A., Falge, E., Aubinet, M., Baldocchi, D., Berbigier, P., Bernhofer, C.,
616 Ceulemans, R., Dolman, H., Field, C., 2002. Energy balance closure at FLUXNET sites.
617 *Agricultural and Forest Meteorology* 113, 223-243.

618

619

List of Figures

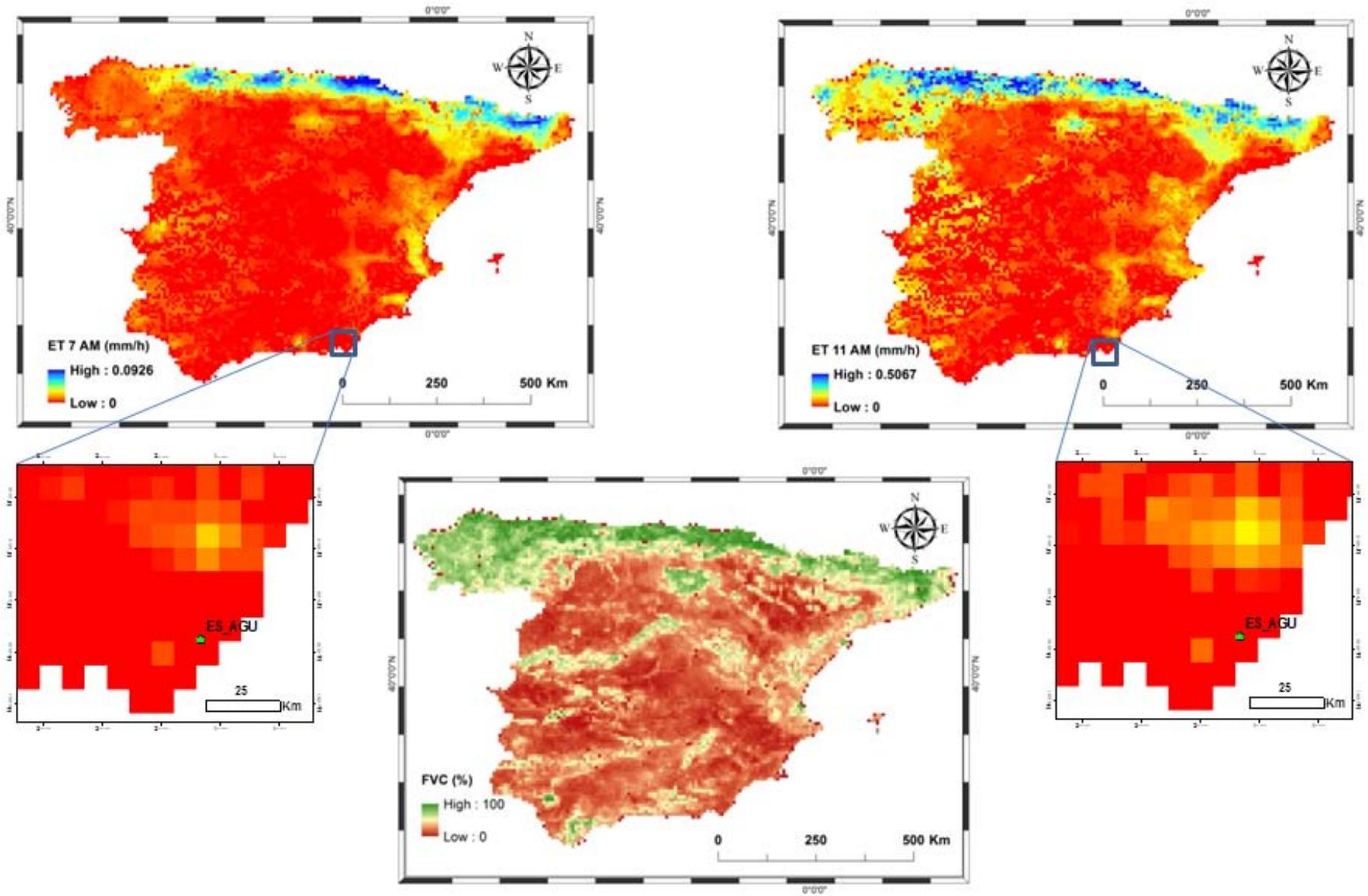


Figure 1: Maps of the SEVIRI ET product on August 6th, 2011 for Spain with the site ES_AGU in the zoomed area. The map in the middle is the map of the Fractional Vegetation Cover as seen from the SEVIRI sensor.

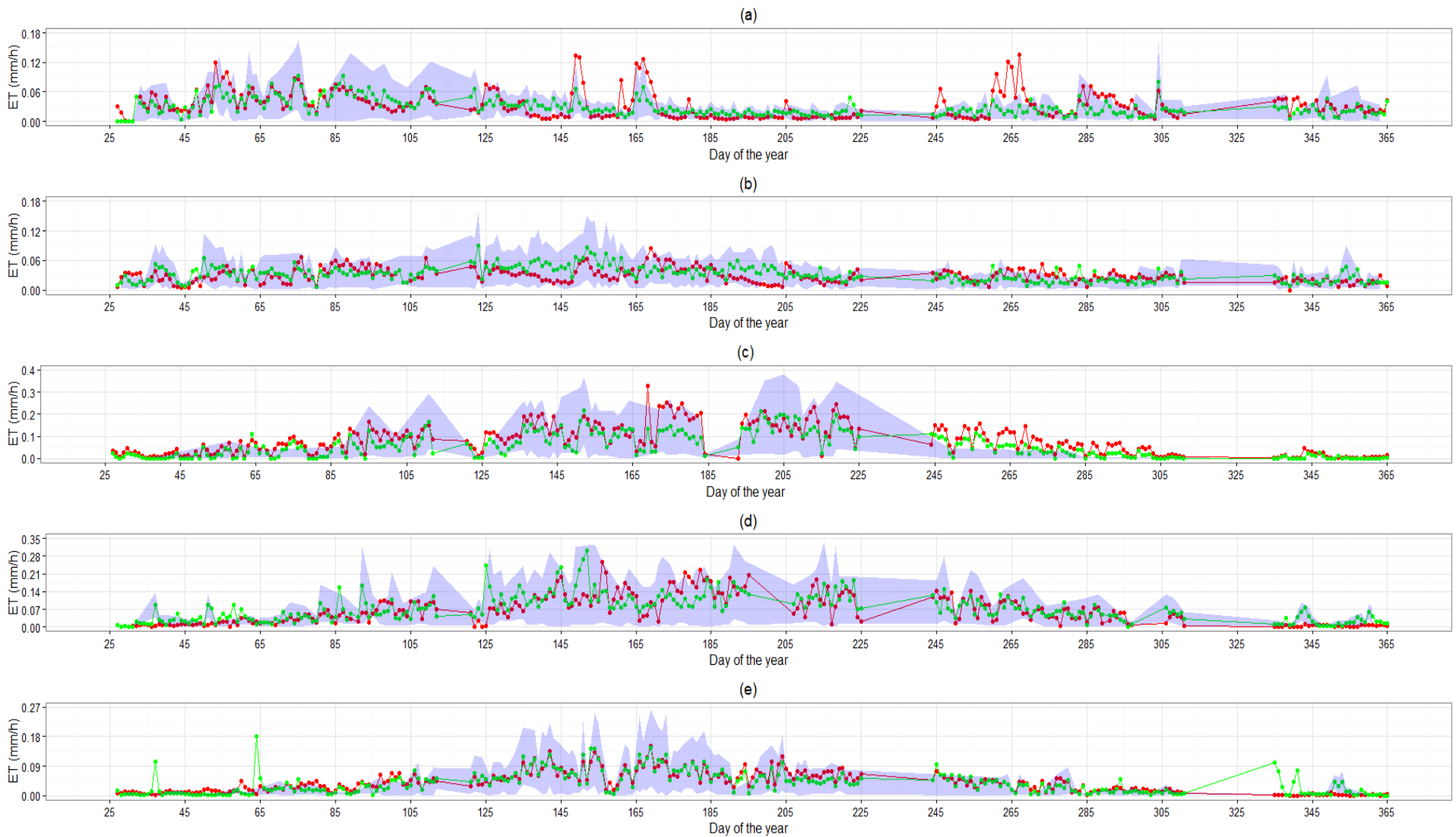


Figure 2a: Examples of the agreement between in-situ and predicted ET from SEVIRI for the different seasons for year 2010 for different sites. In particular, results are shown for: (a) ES_AGU; (b) ES_LJU; (c) IT_CAS; (d) UK_EBU and (e) IT_MBO. Green represents the in-situ ET daily mean, Red is the SEVIRI-predicted ET, Blue is daily standard deviation of the in-situ ET.

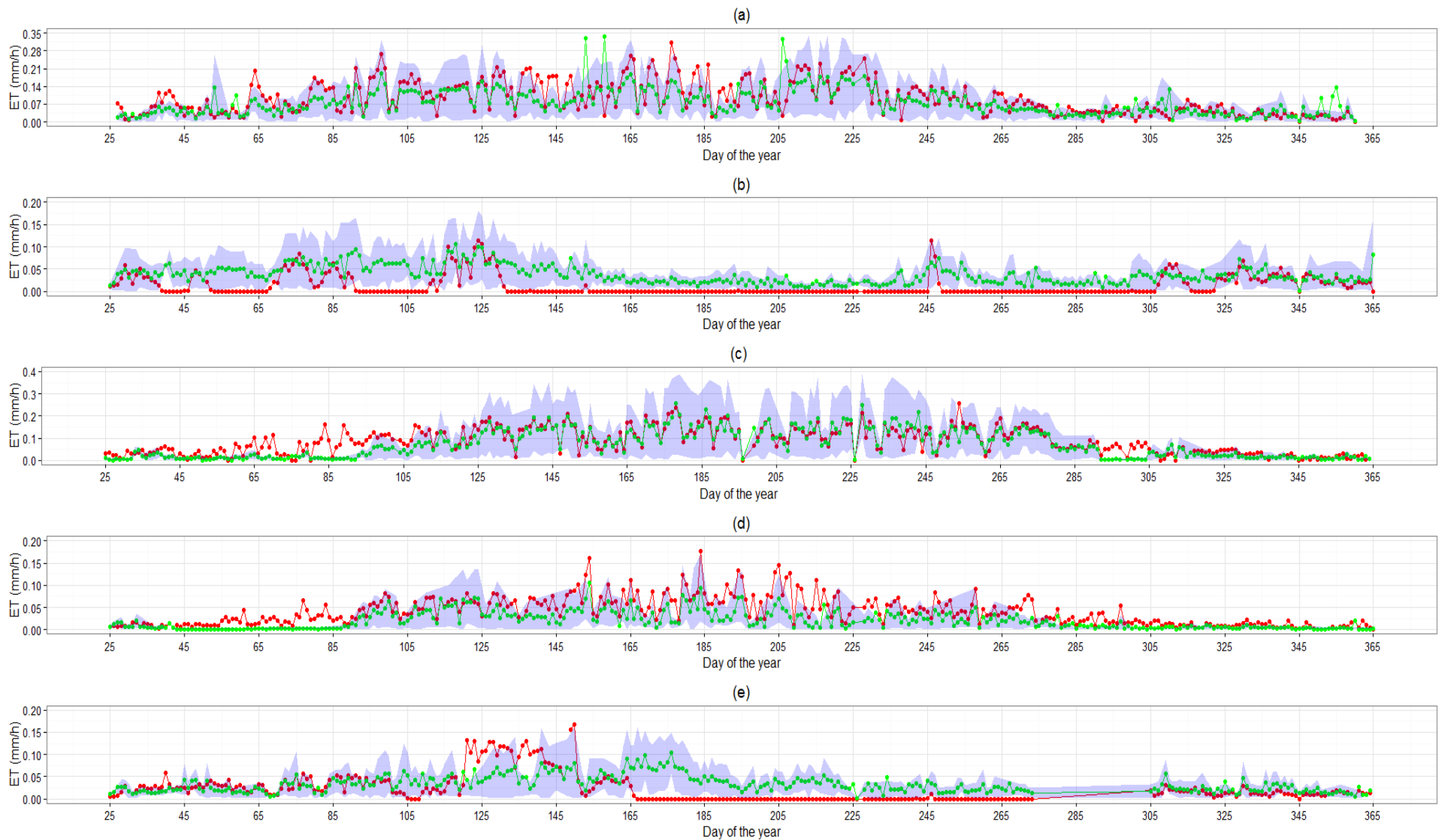


Figure 2b: Examples of the agreement between in-situ and predicted ET from SEVIRI for the different seasons for year 2011 for different sites. In particular, results are shown for: In particular, (a): FR_MAU; (b): ES_AGU; (c):IT_MBO; (d): UK_EBU and (e): ES_LJU. Green represents the in-situ ET daily mean, Red is the SEVIRI-predicted ET, Blue is daily standard deviation of the in-situ ET.

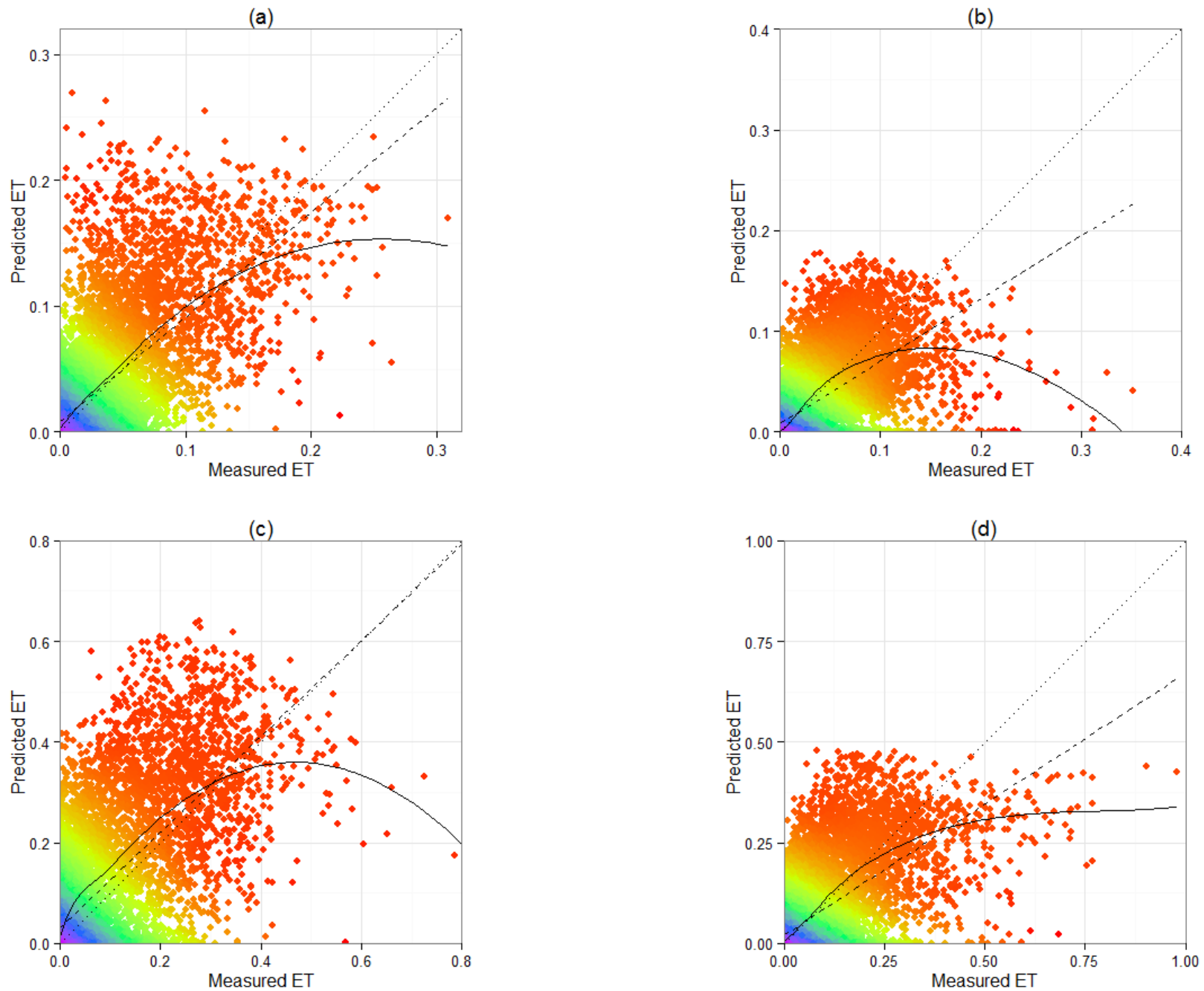


Figure 3a: Agreement between in-situ and predicted ET from SEVIRI for the different seasons for all sites together shown here for year 2010. In particular, (a): autumn, (b)winter, (c): spring and (d): summer; dashed = linear regression, continuous line = locally polynomial (package loess), dotted = $y=x$ line. **Units of ET are in mm h^{-1}**

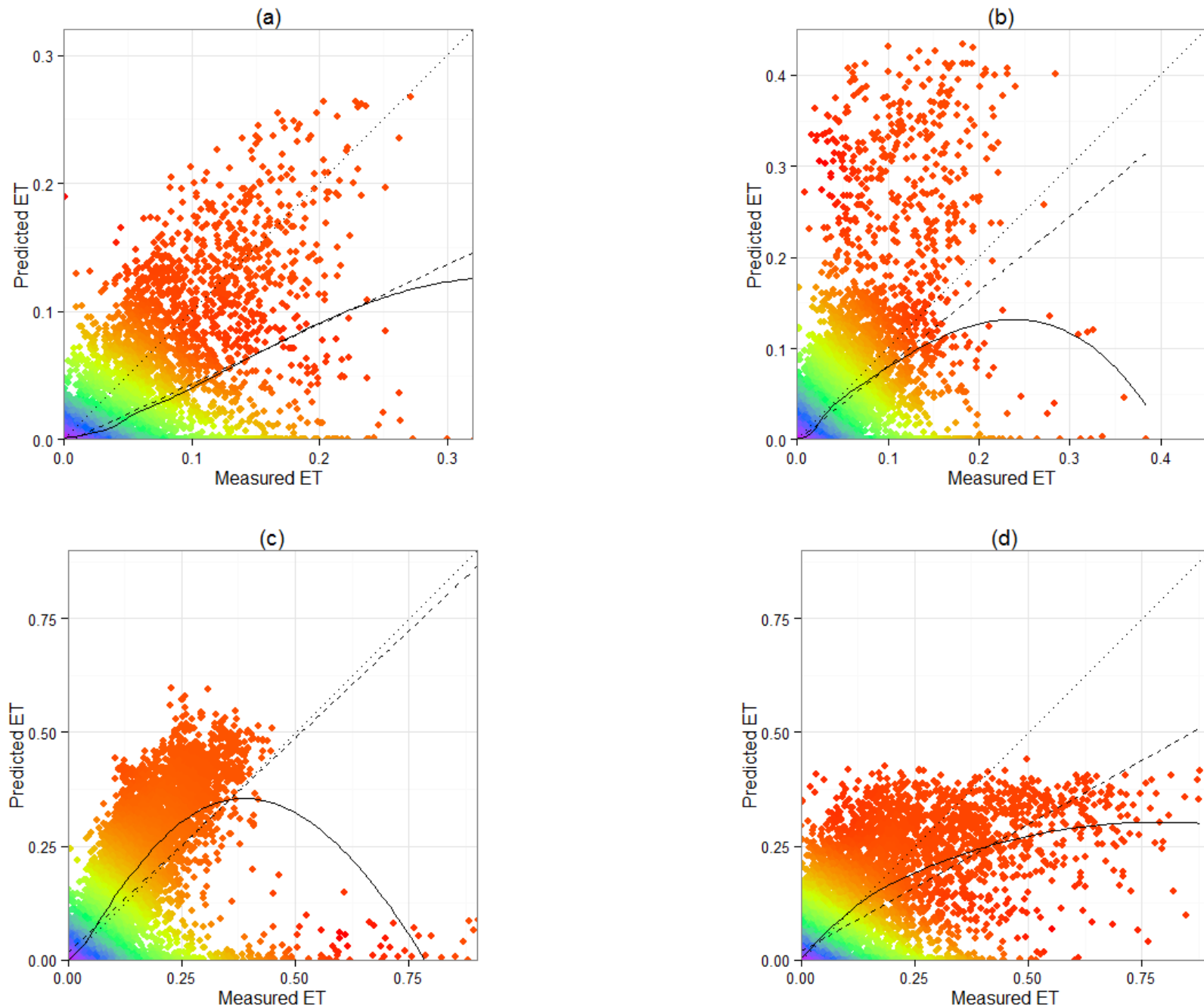


Figure 3b: Agreement between in-situ and predicted ET from SEVIRI for the different seasons for all sites together shown here for year 2011. In particular, (a): autumn, (b)winter, (c): spring and (d): summer; dashed = linear regression, continuous line = locally polynomial (package loess), dotted = $y=x$ line. Units of ET are in mm h^{-1}

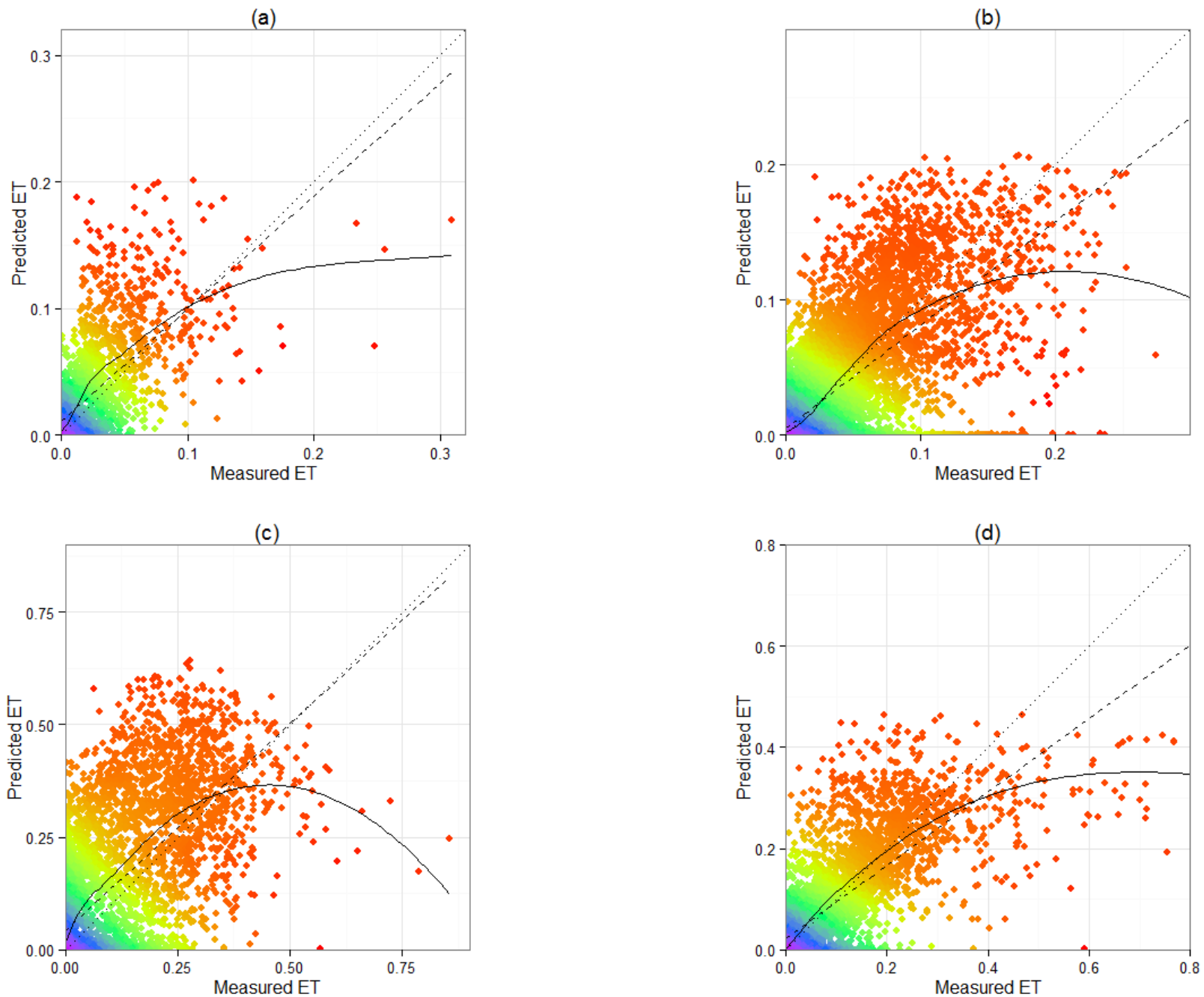


Figure 4a: Agreement between in-situ and predicted ET from SEVIRI for the different Fractional Vegetation Cover (FVC) ranges for all sites together for year 2010. In particular, (a): 0-24% FVC; (b):25-49% FVC; (c): 50-74% FVC and (d): 75-100% FVC; dashed = linear regression, continuous line = locally polynomial (package loess), dotted = $y=x$ line. Units of ET are in mm h^{-1}

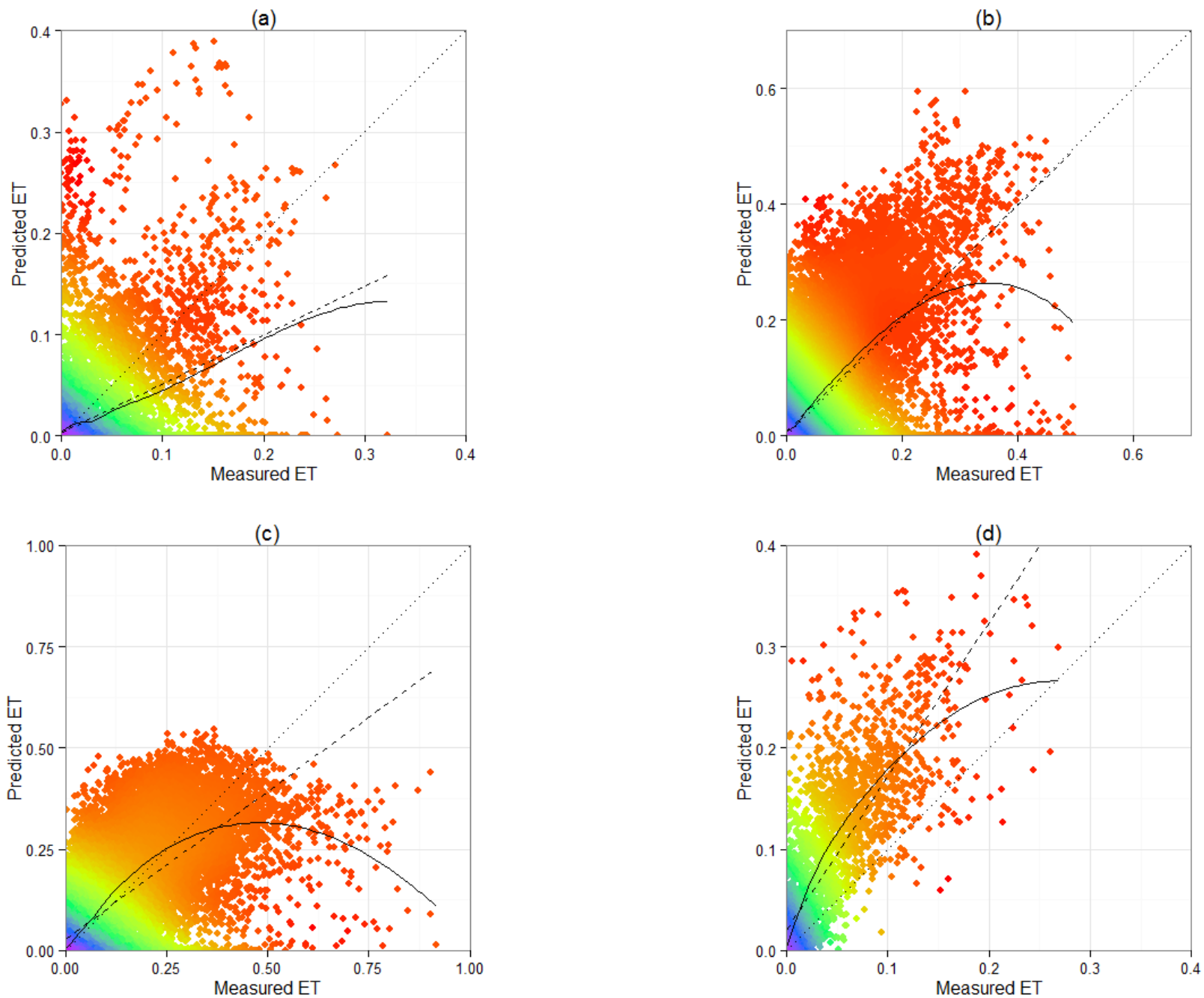


Figure 4b: Agreement between in-situ and predicted ET from SEVIRI for the different Fractional Vegetation Cover (FVC) ranges for all sites together for year 2011. In particular, (a): 0-24% FVC; (b):25-49% FVC; (c): 50-74% FVC and (d): 75-100% FVC; dashed = linear regression, continuous line = locally polynomial (package loess), dotted = $y=x$ line. Units of ET are in mm h^{-1}

Table 1: Description of the selected sites for MSG SEVIRI product validation over Europe

Site Name	Aguamarga	Llano de los Juanes	Renon/Ritten (Bolzano)	Monte Bondone	Castellaro	Mauzac	Easter Bush- Scotland
Site Abbreviation	ES_Agu	ES_LJu	IT_Ren	IT_Mbo	IT_Cas	FR_Mau	UK_EBu
Lat/Long	36.9406/-2.0329	36.9283/-2.7505	46.5878/11.4347	46.0296/11.0029	45.07/8.7175	43.3853/1.2922	55.866/-3.2058
Country	SPAIN	SPAIN	ITALY	ITALY	ITALY	FRANCE	United Kingdom
Vegetation Type	Open Shrublands	Open Shrublands	Evergreen Needleleaf Forests	Grasslands	Croplands	Grasslands	Grasslands
Plant Functional Type	Shrub	Shrub	Evergreen Needleleaf Trees	Annual Grass Vegetation	Cereal crop	Cereal crop	Grass
Climate	Arid Steppe, cold	Warm, temperate, with dry, hot summer	Snow, fully humid, cool summer	Snow, fully humid, warm summer	Warm, temperate, humid with hot summer	Warm, temperate, humid with warm summer	Warm, temperate, fully humid with warm summer
LAI F/PAR Land Cover	Shrubs	Shrubs	Evergreen Needleleaf Forest	Grasses/Cereal Crops	Grasses/Cereal Crops	Grasses/Cereal Crops	Grasses/Cereal Crops
Elevation (m)	195	1622	1794	1547	0	0	208
Dominant Species/Genus	Sumac (<i>Rhus</i>), Toyon (<i>Heteromeles</i>), Coffee berry (<i>Rhamnus</i>) species	<i>Olea europaea</i> , <i>Macchia</i>	<i>Picea</i>	<i>Nardetum alpinum</i>	Cereal Crop	Cereal Crop	C3 grasses

Table 2: Results from land cover type comparison between SEVIRI-predicted and in-situ ET half-hourly estimates ($\text{mm}\cdot\text{h}^{-1}$) for the seven selected sites over Europe in 2010, 2011, both years and a statistical summary for all sites.

Site Abbrev.		ES_Agu	ES_LJu	IT_Ren	IT_Mbo	IT_Cas	FR_Mau	UK_EBu	
Statistical parameter	Year of analysis			Evergreen Needleleaf Forest	Grasses/Cereal Crops	Grasses/Cereal Crops	Grasses/Cereal Crops	Grasses/Cereal Crops	Statistical Summary
		Shrubs	Shrubs						
Bias	2010	0.003	-0.004	-0.007	0.022	0.028		0.003	0.001
	2011	-0.024	-0.007	-0.016	0.013		0.012	0.020	
	both	-0.001	-0.006	-0.012	0.017			0.012	
Scatter	2010	0.035	0.032	0.091	0.078	0.096		0.039	0.065
	2011	0.038	0.050	0.092	0.087		0.085	0.037	
	both	0.035	0.043	0.092	0.084			0.039	
RMSD	2010	0.036	0.032	0.092	0.081	0.100		0.039	0.065
	2011	0.045	0.051	0.093	0.088		0.086	0.042	
	both	0.035	0.044	0.093	0.085			0.041	
MAE	2010	0.022	0.021	0.056	0.054	0.059		0.020	0.037
	2011	0.030	0.057	0.054	0.058		0.047	0.023	
	both	0.021	0.025	0.055	0.057			0.022	
Slope	2010	0.832	0.622	0.650	0.883	0.951		0.785	0.772
	2011	0.466	0.823	0.558	0.785		0.941	1.346	
	both	0.776	0.738	0.591	0.829			0.904	
Intercept	2010	0.008	0.008	0.021	0.031	0.031		0.011	0.012
	2011	-0.003	-0.002	0.019	0.030		0.017	0.013	
	both	0.006	0.003	0.021	0.030			0.015	
r	2010	0.684	0.620	0.644	0.794	0.705		0.801	0.709
	2011	0.546	0.536	0.696	0.706		0.730	0.792	
	both	0.655	0.552	0.669	0.744			0.759	

Table 3: Summary of the comparisons per season between satellite-derived and observed ET estimates ($\text{mm}\cdot\text{h}^{-1}$) in the validation sites for 2010, 2011 and both years.

2010	SEASONS	Bias	Scatter	RMSD	MAE	Slope	Intercept	r
ALL SITES (EUROPE)	AUTUMN	0.006	0.052	0.052	0.030	0.796	0.014	0.706
	WINTER	-0.001	0.037	0.037	0.019	0.403	0.011	0.432
	SPRING	0.007	0.070	0.070	0.040	0.735	0.021	0.658
	SUMMER	0.017	0.091	0.092	0.054	0.903	0.024	0.731

2011	SEASONS	Bias	Scatter	RMSD	MAE	Slope	Intercept	r
ALL SITES (EUROPE)	AUTUMN	-0.005	0.057	0.057	0.032	0.642	0.011	0.685
	WINTER	-0.004	0.041	0.041	0.020	0.272	0.012	0.344
	SPRING	0.013	0.073	0.075	0.046	1.022	0.012	0.707
	SUMMER	-0.008	0.090	0.091	0.056	0.719	0.016	0.707

2010 & 2011	SEASONS	Bias	Scatter	RMSD	MAE	Slope	Intercept	r
ALL SITES (EUROPE)	AUTUMN	0.000	0.055	0.055	0.031	0.686	0.013	0.687
	WINTER	-0.003	0.039	0.040	0.020	0.317	0.012	0.376
	SPRING	0.010	0.072	0.073	0.043	0.877	0.017	0.679
	SUMMER	0.006	0.091	0.092	0.055	0.813	0.021	0.714

Table 4: Agreement between SEVIRI predicted and in-situ ET estimates ($\text{mm}\cdot\text{h}^{-1}$) as a function of Fractional Vegetation Cover (FVC) for the selected sites in 2010 and 2011.

Val. Sites	FVC ranges	Year	Bias	Scatter	RMSD	MAE	Slope	Intercept	r
ES_AGU	FVC 0-0.24	2010	0.009	0.028	0.029	0.016	0.835	0.011	0.663
		2011	-0.013	0.036	0.038	0.023	0.394	0.000	0.545
	FVC 0.25-0.49	2010	0.007	0.035	0.036	0.022	0.824	0.013	0.771
		2011	-0.011	0.038	0.039	0.021	0.278	0.007	0.428
ES_LJU	FVC 0.25-0.49	2010	-0.003	0.029	0.030	0.019	0.759	0.004	0.665
		2011	-0.006	0.047	0.048	0.025	0.822	-0.002	0.535
IT_REN	FVC 0.25-0.49	2010	0.000	0.082	0.082	0.055	0.520	0.034	0.540
		2011	0.009	0.072	0.073	0.043	0.790	0.019	0.620
	FVC 0.5-0.74	2010	0.001	0.108	0.108	0.071	0.642	0.034	0.581
		2011	-0.037	0.108	0.114	0.072	0.512	0.020	0.707
	FVC 0.75-1	2010	-0.004	0.109	0.109	0.072	0.629	0.040	0.686
		2011	-0.008	0.084	0.084	0.056	0.912	-0.002	0.677
IT_MBO	FVC 0.25-0.49	2010	0.043	0.081	0.092	0.117	1.115	0.040	0.487
		2011	0.025	0.066	0.070	0.044	1.058	0.022	0.680
	FVC 0.5-0.74	2010	0.008	0.084	0.084	0.060	0.905	0.021	0.833
		2011	0.000	0.106	0.106	0.078	0.745	0.033	0.692
UK_EBU	FVC 0.25-0.49	2010	0.000	0.033	0.033	0.019	0.838	0.007	0.818
		2011	0.022	0.037	0.043	0.024	1.454	0.025	0.645
	FVC 0.5-0.74	2010	0.005	0.033	0.034	0.022	1.030	0.003	0.910
		2011	0.015	0.036	0.039	0.025	1.021	0.014	0.787
	FVC 0.75-1	2010	-0.001	0.036	0.036	0.023	0.859	0.008	0.890
		2011	0.038	0.052	0.064	0.042	1.470	0.021	0.795
IT_CAS (2010)	FVC 0.25-0.49	2010	0.024	0.074	0.077	0.045	0.884	0.028	0.632
	FVC 0.5-0.74	2010	0.035	0.117	0.122	0.079	0.919	0.043	0.683
FR_MAU (2011)	FVC 0.25-0.49	2011	0.010	0.079	0.079	0.043	0.914	0.016	0.727
	FVC 0.5-0.74	2011	0.024	0.101	0.104	0.063	1.029	0.021	0.755

Table 5: Summary of the agreement between SEVIRI predicted and in-situ ET estimates (mm.h⁻¹) as a function of Fractional Vegetation Cover (FVC) in 2010 and 2011.

Val. Sites	FVC ranges	Year	Bias	Scatter	RMSD	MAE	Slope	Intercept	R
ALL SITES (EUROPE)	FVC 0-0.24	2010	0.009	0.028	0.029	0.016	0.835	0.011	0.663
		2011	-0.008	0.044	0.044	0.026	0.445	0.004	0.430
		Both	-0.005	0.042	0.042	0.024	0.470	0.006	0.445
	FVC 0.25-0.49	2010	0.011	0.056	0.057	0.032	0.813	0.017	0.611
		2011	0.003	0.064	0.064	0.036	0.910	0.007	0.674
		Both	0.005	0.061	0.061	0.034	0.882	0.010	0.658
	FVC 0.5-0.74	2010	0.018	0.106	0.108	0.071	0.845	0.034	0.705
		2011	-0.005	0.103	0.103	0.066	0.694	0.029	0.690
		Both	0.006	0.105	0.105	0.068	0.757	0.032	0.692
	FVC 0.75-1	2010	-0.002	0.071	0.071	0.041	0.723	0.021	0.773
		2011	0.036	0.054	0.065	0.042	1.373	0.023	0.771
		Both	0.014	0.067	0.069	0.041	0.753	0.030	0.735